Medical Hypotheses 132 (2019) 109360

Contents lists available at ScienceDirect

Medical Hypotheses

journal homepage: www.elsevier.com/locate/mehy

Toward a closed-loop deep brain stimulation in Parkinson's disease using local field potential in parkinsonian rat model

Sana Amoozegar[a], Mohammad Pooyan[a,*], Mehrdad Roughani[b]

[a] Department of Biomedical Engineering, Faculty of Engineering, Shahed University, Tehran, Iran
[b] Department of Physiology, Faculty of Medical Sciences, Shahed University, Tehran, Iran

ARTICLE INFO

Keywords:
Parkinson's disease
Closed-loop deep brain stimulation
Local field potential
High frequency features
Genetic algorithm
Support Vector Machine

ABSTRACT

Deep brain stimulation (DBS) is an invasive method used for treating Parkinson's disease in its advanced stages. Nowadays, the initial adjustment of DBS parameters and their automatic matching proportion to the progression of the disease is viewed as one of the research areas discussed by the researchers, which is called closed-loop DBS. Various studies were conducted regarding finding the signal(s) which reflects different symptoms of the disease. Local Field Potential (LFP) is one of the signals that is suitable for using as feedback, because it can be recorded by the same implemented electrodes for stimulation. The present study aimed to identify the distinguishing features of patients from healthy individuals using LFP signals.

Methods: In the present study, LFP was recorded from the rats in sham and parkinsonian model groups. After evaluating the signals in the frequency domain, sixty-six features were extracted from power spectral density of LFPs. The features were classified by Support Vector Machine (SVM) to determine the ability of features for separating parkinsonian rats from healthy ones. Finally, the most effective features were selected for distinguishing between the sham and parkinsonian model groups using a genetic algorithm.

Results: The results indicated that the frequency domain features of LFP signals from rats have capacity of using them as a feedback for closed-loop DBS. The accuracy of the Support Vector Machine classification using all 66 features was 80.42% which increased to 84.41% using 38 features selected by genetic algorithm. The proposed method not only increase the accuracy, but it also reduce computation by decreasing the number of the effective features. The results indicate the significant capacity of the proposed method for identifying the effective high-frequency features to control the closed-loop DBS.

Conclusions: The ability of using LFP signals as feedback in closed-loop DBS was shown by extracting useful information in frequency bands below and above 100 Hz regarding LFP signals of parkinsonian rats and sham ones. Based on the results, features at frequencies above 100 Hz were more powerful and robust than below 100 Hz. The genetic algorithm was used for optimizing the classification problem.

Introduction

Parkinson's disease (PD) is regarded as a progressive and irreversible disease which has no permanent cure. The current treatments mainly focus on decelerating the progression of the disease, controlling its symptoms, and improving the quality of life of the patients [1]. PD is a neurodegenerative disease characterized, in part, by the death of dopaminergic neurons in the substantia nigra (SN) pars compacta [2]. Dopamine which transmits neural signals from the substantia nigra to the striatum, is secreted by dopaminergic neurons of the midbrain in the mammalian central nervous system [3]. The SN is a basal ganglia structure located in the midbrain that plays an important role in movement [4]. Neural signals balance the body movement while other responsible centers for controlling body movement act irregularly by the destruction of dopaminergic neurons in the SN. Clinical symptoms of PD appear in advanced stages with the destruction of 80% of the dopaminergic neurons [5]. DBS is considered as one of the effective invasive methods used for treating advanced PD. Deep stimulation of certain areas of the brain aims to treat therapy-resistant and passive movement disorders [6,7]. In fact, DBS is generated by a system, the electrodes of which are mainly implanted in a region of the brain called the subthalamic nucleus (STN) by a complex surgery, and thus it can reduce the effects of the disease and improve the patient's state by applying DBS. Despite the apparent effect of DBS on neurological diseases, especially PD, this method still needs to be optimized in order to be more effective in treating the disease. The current trend of DBS is

* Corresponding author.
E-mail address: pooyan@shahed.ac.ir (M. Pooyan).

https://doi.org/10.1016/j.mehy.2019.109360
Received 11 July 2019; Received in revised form 4 August 2019; Accepted 11 August 2019

based on open-loop structure and fixed stimulation parameters. Therefore, rapid clinical symptom variations and motor fluctuations of PD patients are approximately uncontrollable and thus different studies have recently been conducted to identify closed-loop DBS systems [8]. In closed-loop DBS, stimulation is applied in a manner compatible with the patient's state including the physical activity, body position, sleep/awakening cycle, and the overall progression of disease using one or more feedback signal(s) which represent the state of the system. While, in open-loop DBS, the stimulator is permanently performed by fixed parameters regardless of the patient's state. At present, initial stimulation settings are normally performed by the skilled neurologist after the implantation of DBS electrodes and then reprogramming is possibly conducted six months after reaching the convincing results [9]. In open-loop stimulation method, the stimulation parameters are subsequently performed manually and only during periodical of 3–12-month programmed visits and DBS settings remain unchanged between these periods, though, the patient experiences an unpleasant event or fluctuation [8]. Accordingly, adaptive system is presented to solve this problem, which includes a simple closed-loop model in which the patient's clinical status is reflected by measurable biomarker and then new stimulation settings are generated and transmitted to the smart implanted pulse generator. The selection of an optimal control variable (biomarker) for providing feedback is regarded as the most essential issue in a closed-loop system [8]. There is no need to complete the programming period since closed-loop DBS stimulator can automatically adapt the DBS settings to the patient's state. This is of great importance, especially for patients who are away from DBS specialized medical centers [10]. Selecting one or more signal(s) to be used as feedback for the system is the first step in creating a closed-loop system. To this end, it is noteworthy that the electrodes, pulse generator, and the extension should be implanted in the body during the DBS surgery while none of them should be physically available after the surgery. In addition, the signal which is taken into account as the feedback should have the ability to reflect the patient's condition toward the system so that to adjust the control parameters accordingly. So far, researchers have utilized various signals to respond to the patient's condition. Action potentials (APs), ECoGs, LFP, and electroencephalogram (EEGs) are examples of electrophysiological biomarkers used in closed-loop DBS systems [11]. LFP is an electrophysiological signal which is the entire temporal-spatial action potential of several adjacent neurons in a small volume of the nerve tissue. LFP signals can be recorded by the implanted microelectrode for DBS, which reflect the synchronized presynaptic and postsynaptic activity of a collection of local neurons that oscillate in response to the patient's clinical state [12]. Priori et al. [13] proposed the first overall structure for closed-loop DBS system.

Among the available feedbacks, the beta-band oscillations from the LFP signal are mostly used [14–17]. Basu et al. [18] utilized the electromyography signal as feedback. Additionally, Kent et al. [19,20] evaluated the characteristics of direct response of the tissue to stimulation employing electrically evoked compound action potentials to the brain of the cat while Gmel et al. [21] used the same signals in the brain of the human being. Gmel et al. [22] used a new signal as a biomarker and recorded the responses which were evoked through the implanted electrodes in the brain of two patients.

Research over the past fifteen years has emphasized that the measured LFP obtained from the STN neurons oscillations can be utilized as the control variable [15,16,23–32]. The fact that LFP signals are simply measured using an electroencephalogram amplifier which is connected to a single contact (mono-polar recording) or two contacts (bipolar recording) in DBS implanted electrodes, is the first reason that LFP is applied as a feedback biomarker for controlling closed-loop DBS [33]. Additionally, the current evidence supports the hypothesis of the dependence of LFP changes on behavioral and cognitive functions. Accordingly, using LFP in closed-loop DBS can control the unwanted changes in the involved oscillations of such functions and reduce the complexity of non-motor cognitive and behavioral impairments [8].

The present study attempted to find biomarkers and looked into their potential in order to develop the closed-loop feedback system. LFP signal of rats were used as a control signal in this research, thus rats preparation for data recording and preprocessing will be described in the following. Processing methods on recording LFP signals will be elaborated next, and selected features from LFP signals which are shown to be remarkably potent will be introduced ultimately.

Materials and methods

Data acquisition

The present study was implemented on 33 male rats (25 Parkinsonian rat model and 8 sham rats) with a weigh of 250–330 g in the laboratory center of Shahed University. The animals were kept in a controlled in vitro environment with sufficient food and water at an average temperature of 21 ± 2 °C and a 12:12 h light–dark cycle. The rats were first anesthetized by injecting ketamine at a dose of 80 mg/kg, i.p. and xylazine at a dose of 8–10 mg/kg, i.p. The depth of anesthesia was adjusted according to the heart rate and hind leg pinch reaction. The animals were fixed in a stereotaxic frame. The skull was exposed by an incision of the scalp with a surgical blade. A burr hole was opened over the left parietal cortex by means of a mini-drill at coordinates 3 mm lateral and 0.2 mm anterior to bregma and ventrally 5 mm below the dura (Fig. 1). For development of PD model, the neurotoxin 6-hydroxydopamine (6-OHDA) was microinjected into the left striatum of rats under anesthesia. The 6-OHDA group received 5 µl of cold normal saline containing 2.5 µg/µl of 6-OHDA-HCl and 0.2% ascorbate. The same surgical operation was performed in the sham group. The sham group received intrastriatal ascorbate-normal saline solution. Four stainless steel screws were attached to the anterior frontal bone and posterior parietal bone in order to fix the dental acrylic firmly. In order to record the LFP signal, three electrodes made of Teflon-coated stainless steel wire (a bare diameter of 127 µm and a coated diameter of 203.2 µm), twisted together. Another hole was opened over the left parietal cortex by means of a mini-drill. Twisted electrodes were implanted (at 3.6 mm posterior and 2.5 mm lateral, and ventrally 8 mm below the dura (Fig. 1)) and then fixed to telecom connector with telecom pins and secure in the surgery site by the dental acrylic.

After two hours of surgical operations including microinjections (6-OHDA-saline), the electrode implantation and fixation, and recovery from anesthesia, the animals were transferred to rat room. Further, a week after the surgery, the 6-OHDA-lesioned rats were injected with apomorphine to ensure model establishment. Fig. 2 shows the surgical process step-by-step. Ethical approval was obtained from the local

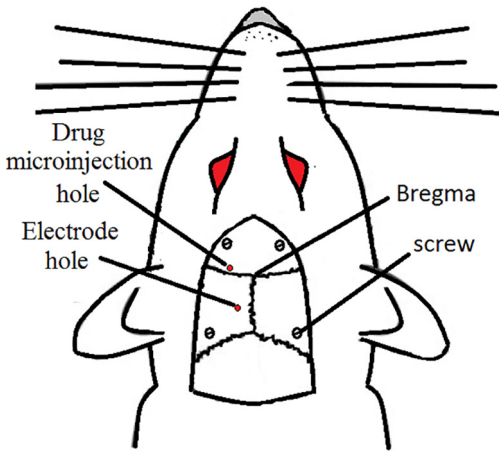

Fig. 1. Schematic illustration of rat preparation showing the location of microinjection, Electrode implantation, bregma and screws locations.

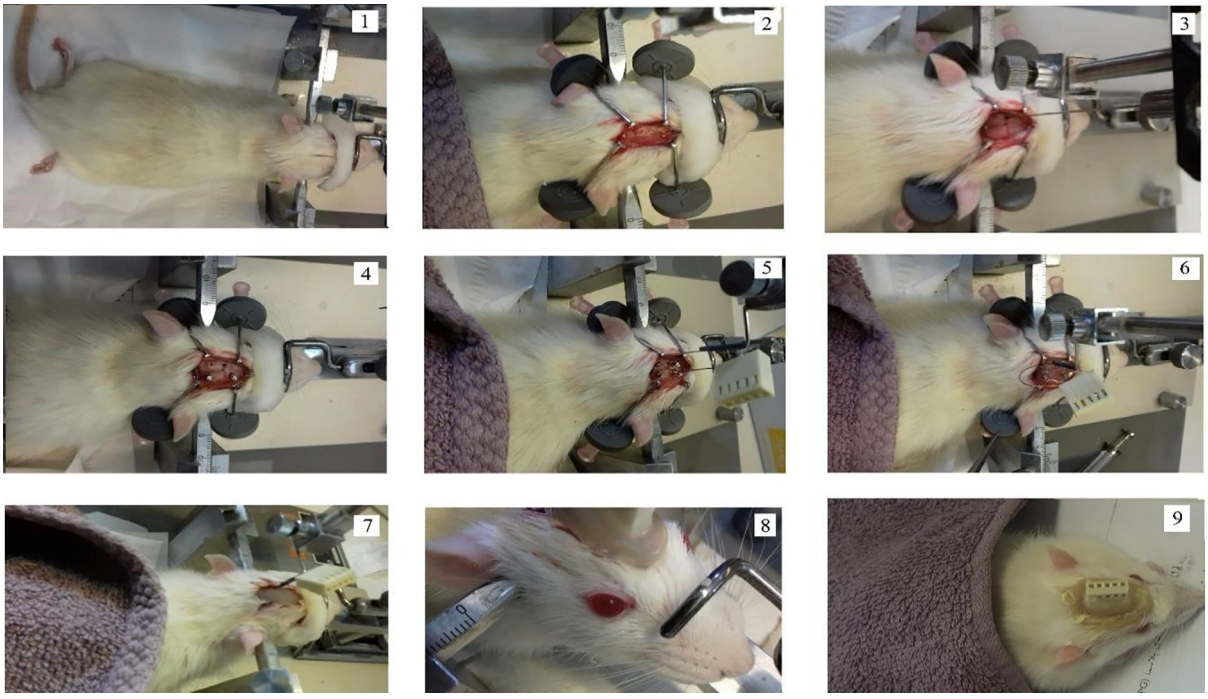

Fig. 2. Surgical procedures, electrode implantation and telecom pins fixations are shown from 1 to 9 subsequently.

ethics committee of Shahed University with code of IR.SHAHED.REC.1398.039.

After one week following verification of model establishment, three implemented electrodes were used for stimulating and recording the signal with respect to the ground electrode which was attached to one of the screw fixed in skull of the rat. The Electromodule R12 Stimulator (Science beam Company) was utilized to simultaneously stimulate DBS and record the LFP signal. The stimulation current was applied to the brain of the rat as a pulse wave (monophasic) with adjustable stimulation parameters as frequency, amplitude, pulse duration, and number of pulse repetition per second. The interval of the applied stimulation parameters is provided in Table 1.

Fig. 3 shows the complete scheme of this study. The LFP signal from the STN of the rats was recorded in three conditions encompassing the recorded LFP signal from the rat brain in the sham group, the LFP signal from 6-OHDA rat models with no stimulation (Off-Stimulation), and the recorded LFP signal from the 6-OHDA-lesioned rats after the stimulation.

According to the parameters in Table 1 a total of 1861 different stimulation conditions were applied to the 6-OHDA-lesioned rats and their LFP signals were recorded and processed (stimulation group). Additionally, the LFP signal of the sham group was recorded on several days and hours. In the Off-Stimulation group, the signals were first recorded from 6-OHDA-lesioned rats before performing any stimulation to the rats.

The recorded dataset was the LFP of neural activity around the recorded electrodes with respect to the reference electrode, that is, the wire which was attached to the skull of the rat. These signals were recorded and stored on the computer by the recorder, which was connected to the computer, and then converted to the format which could be processed by Matlab software. The idea of recording signals in sham, Off-Stimulation, and stimulation groups was derived from a rational expectation regarding improving the motor parameters of the Parkinsonian patients after receiving deep brain stimulation. It was expected that the extracted features from the signals of stimulation group get closer to the obtained features of the sham group. The recorded signals obtained from the Off-Stimulation group aimed to help to find features which make a significant distinction between the sham group and 6-OHDA-lesioned rats. In addition, the stimulation parameters alteration in the stimulation group simultaneously leads to the proximity of its features to those in the sham group. Therefore, features with 2 characteristic are of great significance: 1) significantly differentiate between sham and Off-Stimulation groups and 2) the extracted features in the stimulation group should involve the features of the two previous groups. In other words, attempts were made to demonstrate that Parkinson's disease disrupts the generated brain signals, and stimulation leads to a change in brain signal characteristics, which is related to various stimulation parameters. Further, some of these stimulation parameters are more able to close the measured features of the stimulation group to the desired features of the sham group. In fact, this stimulation protocol makes the state of Parkinson's rat model close to the healthy rat. Fig. 4 illustrates an example of the recorded signals in the three groups under investigation.

Table 1
The Range and Resolution of Variations in Stimulation Parameters.

Stimulation Parameter	Variation Interval	Variation Resolution
Frequency	110–150 (Hz)	5 (Hz)
Amplitude	1, 10, 20–300 (μA) (extending the range to the point that the side effects are detected)	20 (μA)
The duration of pulse	20–100 (μs)	20 (μs)
The number of pulse repetition	10–70	20

LFP signal preprocessing

Fig. 4 display the data samples in three different groups. These data are raw and require initial processing for further investigation. The frequency domain analysis of the brain signal is considered as one of the selected topics in studies related to patients with PD. Furthermore, beta-band oscillations in the LFP signal have been previously used as a biomarker in PD. Therefore, in the present study LFP signals at a sampling rate of 10 kHz were evaluated in the low-frequency band; below 100 Hz and high frequency band; above 100 Hz. A Chebyshev

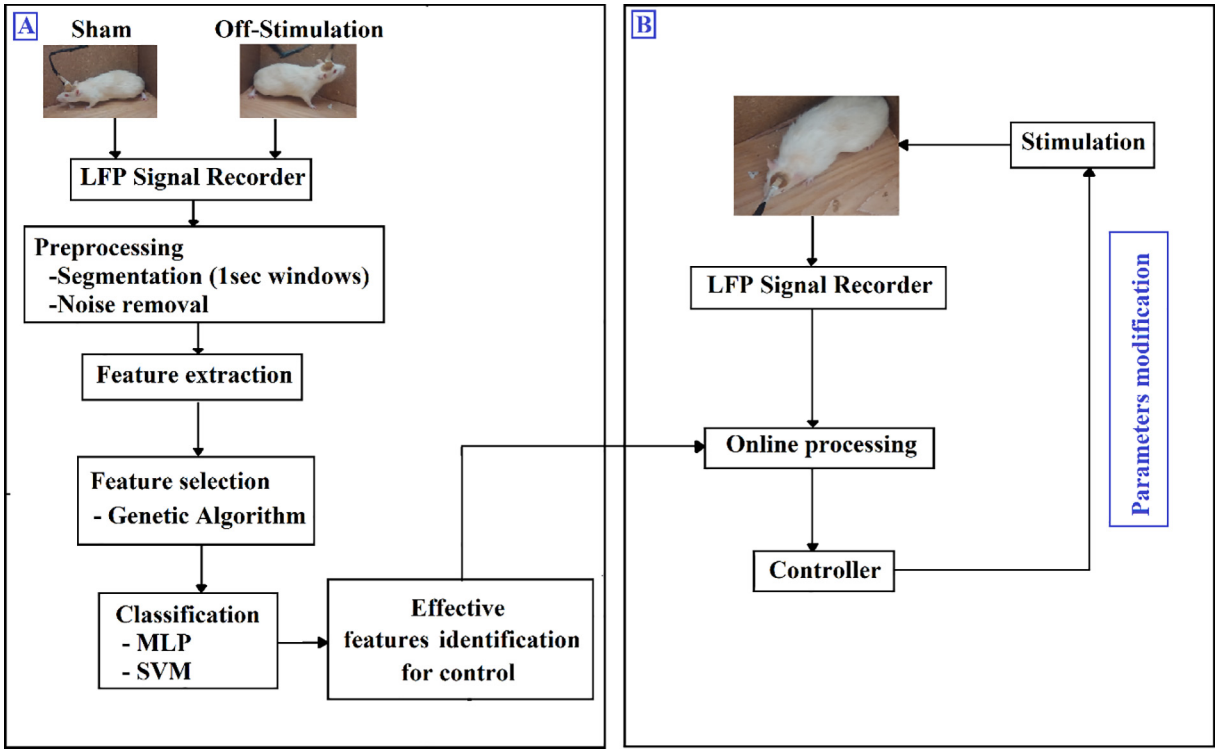

Fig. 3. The complete scheme of the present research. A) Offline processing to identify the effective features using as feedback in further closed-loop DBS system. B) Online Closed-loop DBS schematic with online processing which controls stimulator by the extracted features from offline processing.

(Type-I) high- and a low-pass filters were employed to separate the high frequency band (above 100 Hz) and low frequency band (below 100 Hz) of signals respectively. Also a Notch filter was used to eliminate the noise of 50 Hz mains power. Further processing was separately applied to the filtered data.

Power spectrum analysis

The Fourier transform was utilized for both high- and low-frequency band of datasets in order to transfer the data from the time domain to the frequency domain, the result of which is shown in Fig. 5 for datasets in sham and Off-Stimulation groups.

The results demonstrate lower amplitude range of high frequency signals compared to the low frequency band, and the large number of local maxima in the Fourier transform of the dataset in both high and low frequency, indicating that the results cannot be generalized to all datasets. Therefore, the power spectrum of the signals was obtained to comprehensively analyze and smooth the dataset frequency information. After applying preprocessing, in order to comprehensively analyze the data and display the overall frequency activity in sham and Off-Stimulation groups power spectral density (PSD) was obtained in low- and high-frequency using the Burg and MUSIC methods, respectively. The results of power spectrum extraction are depicted in Fig. 6.

The following features were extracted after obtaining the PSD of all signals.

The extracted features related to the power spectrum of low-frequency signals were as follows:

1. The amplitude of seven local maxima available in the power spectrum, sorted by the largest one;
2. The normalized amplitude of seven local maxima available in the power spectrum , sorted by the largest one;
3. The location of occurrence of seven local maxima (frequency of each local maximum);
4. The amplitude of seven local maxima available in the power spectrum, ranked based on occurrence (seven low frequencies);
5. The location of occurrence of seven local maxima in stage four;
6. The number of local maxima, the amplitude of which is greater than 1/14 of the total maximum;
7. The average of the normalized power spectrum amplitude;
8. The area under PSD curve (signal energy).

Similarly the extracted features respecting the power spectrum of high-frequency signals are as follows:

1. The amplitude of five local maxima available in the power spectrum, sorted by the largest one;
2. The normalized amplitude of five local maxima available in the power spectrum , sorted by the largest one;
3. The location of occurrence of five local maxima (frequency of each local maximum(;
4. The amplitude of five local maxima available in the power spectrum, ranked based on occurrence (seven low frequencies);
5. The location of occurrence of five local maxima in stage four;
6. The number of local maxima, the amplitude of which is greater than 1/14 of the total maximum;
7. The average of the normalized power spectrum amplitude;
8. The area under PSD curve (signal energy. (

Thus 38 and 28 features were extracted from low- and high-frequency domains of the datasets respectively, and a total of 66 features were obtained from each signal. Considering the best features make the most distinction between the sham and Off-Stimulation groups, feature selection methods are needed to select best mixture of features and an appropriate classifier is required to best classify sham and Off-Stimulation groups. Based on various trials, the current study used the genetic algorithm (GA) for feature selection and Support Vector Machine (SVM) for classification as are explained in the following.

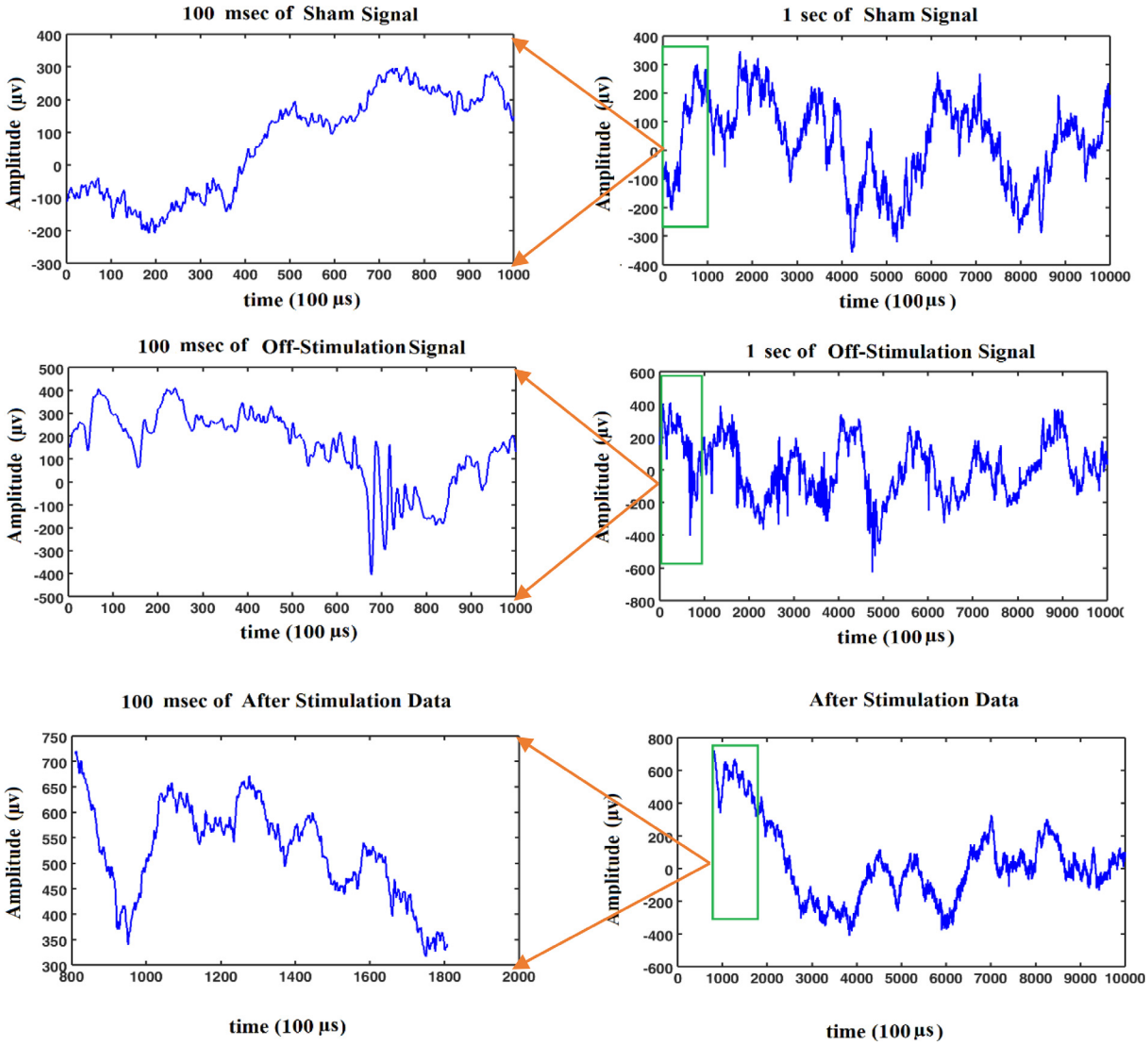

Fig. 4. Sham, Off-Stimulation and stimulation LFP signals samples (left-hand figures are the magnified versions of the right ones).

Feature selection

Genetic algorithm

The GA is an adaptive innovative search method which is inspired by natural selection and genetic principles. GA begins with a primary population of chromosomes, each of which is a possible solution for an optimal problem and proceeds to a more optimal collection of chromosomes. Chromosomes contain continuous or discrete numerical values (strings), especially bit strings. The process of improvement is performed by three general actions including selection, crossover, and mutation. Based on the value of the fitness score, GA selects the best chromosomes from the current population, which were called parents, allowing these chromosomes to move to the next stage. Crossover indicates the combination of two chromosomes such that parents are allowed to substitute their genes together and transfer the new chromosomes, which are called the child, to the next generation. A part of this new population is created through mutation which a random change occurs in the genes of the parent in order to cover the whole population. Fig. 7 illustrates crossover and mutation operations on the chromosomes. Each chromosome has eight genes, and each gene can have a value equal to 1 or 0 (means that the feature selected or not).

Classification

In this work, two classifiers, Support Vector Machine (SVM) and Multilayer Perceptron (MLP), were compared to differentiate between the sham and patient groups. To flag problems like overfitting and selection bias, a cross-validation method was applied on data. At each stage, 30% of the observations was selected randomly as the testing data and the other remaining 70% as the training data. To achieve the average accuracy, sensitivity and specificity, the above process was repeated 10 times.

Multilayer perceptron (MLP)

The applied MLP was made of a three-layer Perceptrons. The input layer had the same number of nodes as the input's vector length. The output layer, on the other hand, contained one node because of 2-class classification problem. Additionally, a large number of neurons in the hidden layer were examined and trained, leading us to the optimized number being 5. It is worth mentioning that the training process has solely been conducted on the training data. Once the training error has dropped to a minimum, we moved on to test the network using the testing data. In fact, never has the data network observed the testing data till selecting the optimal structure, which brings an improvement on the proper generalization of the network [34–40]. It should be noted

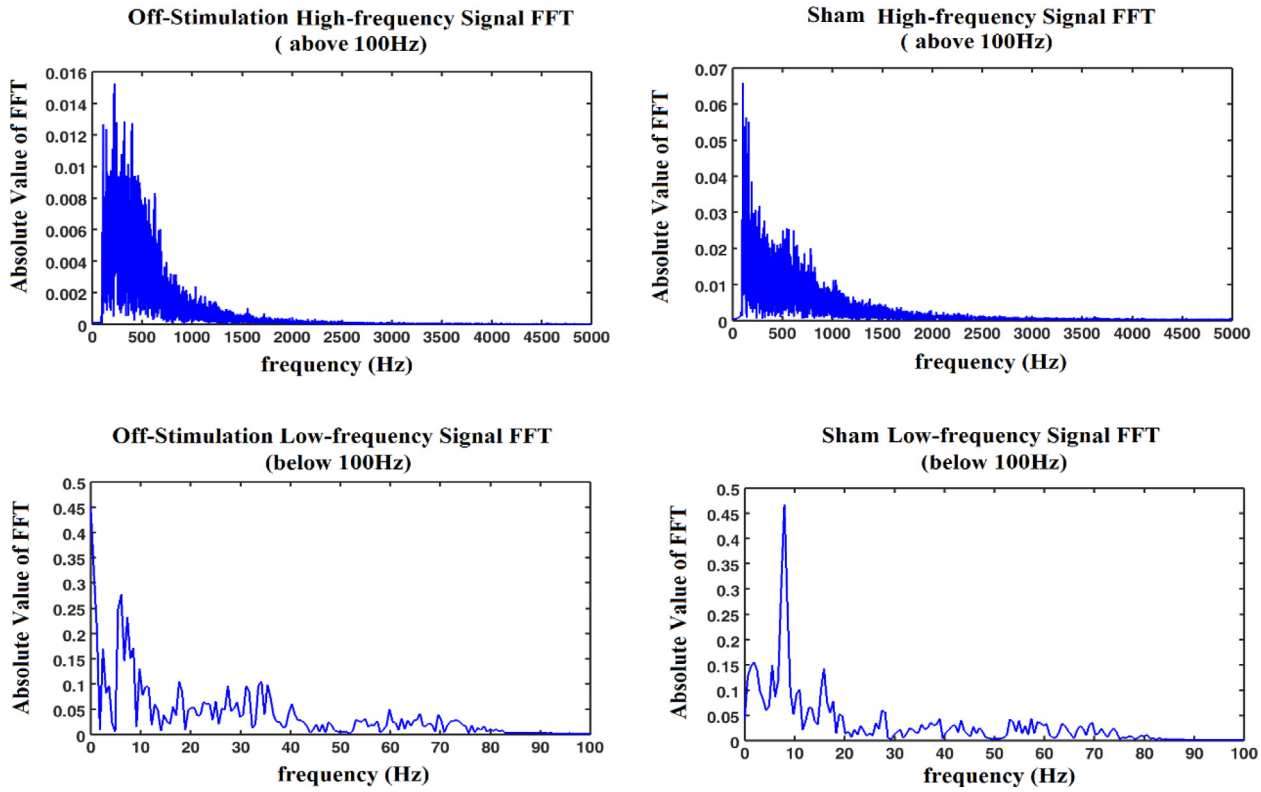

Fig. 5. An example of Fourier transform on high-frequency and low-frequency data for sham and Off-Stimulation groups.

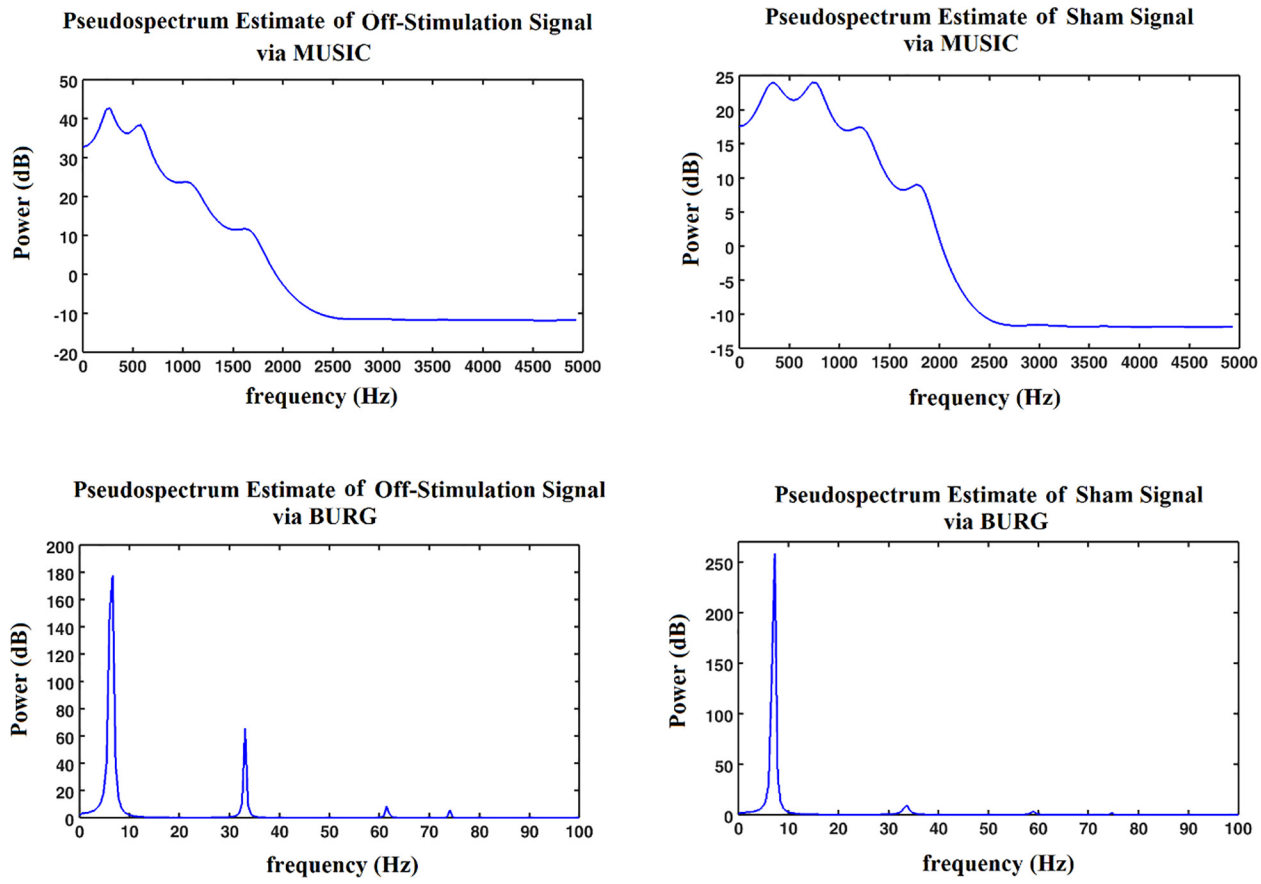

Fig. 6. An example of the power spectrum of high and low frequency datasets of both sham and OFF stimulation groups using MUSIC and BURG methods.

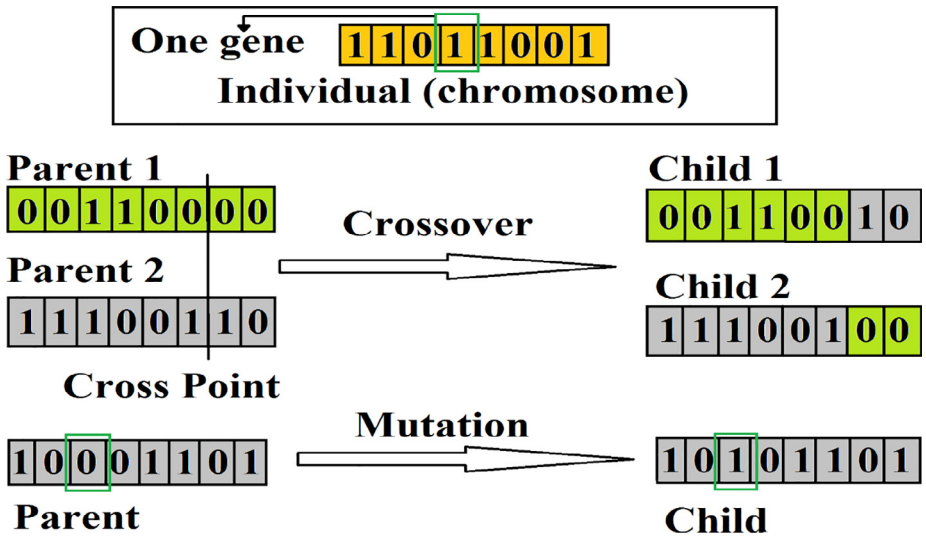

Fig. 7. Crossover and mutation operations in genetic algorithm.

that the output and the hidden layer had a linear transfer function and a tangent sigmoid function, respectively. Network training proceeded until the mean value of error was less than 0.01, or the number of training iterations reached 1000.

Support Vector Machine

SVM is a well-known supervised learning model that analyzes data used for classification and regression. SVM learns a linear model which can divide the data into two parts. In fact, SVM finds the best hyper plane that separates the data related to both classes with the maximum margin. In problems which the data cannot be linearly separated, the data (from the N-dimensional input space) are mapped, through some nonlinear mapping, to a space with a larger dimension (M-dimensional feature space M > N), where the data classes can be linearly separated. In other words, the SVM is an extension of nonlinear models of the generalized portrait algorithm based on statistical learning theory. The goal of regression is to determine the best model from a set of models (named Estimating Functions) to approximate future values accurately. The generic support vector regression estimating function is:

$$f(x) = (w \cdot \Phi(x)) + b \tag{1}$$

where $w \subset R_n$, $b \subset R$ and Φ is a nonlinear function that maps x into a higher dimensional space. W and b are the weight vector and bias, respectively. The weight vector (w) can be written as:

$$w = \sum_{i=1}^{L} (\alpha_i - \alpha_i^*) \tag{2}$$

By substituting Eq. (1) into Eq. (2), the generic equation can be rewritten as:

$$f(x) = \sum_{i=1}^{L} (\alpha_i - \alpha_i^*)(\Phi(x_i) \cdot \Phi(x)) + b \tag{3}$$

$$f(x) = \sum_{i=1}^{l} (\alpha_i - \alpha_i^*)\, k(xi.x) + b \tag{4}$$

In Eq. (4), the function $k(x_i.x) = (x_i).\Phi(x))$ is replaced with the dot product and is known as the kernel function and $\alpha = (\alpha 1, \alpha 2, \ldots, \alpha l)$ the vector of nonnegative Lagrange multipliers.

The choice of kernel functions and kernel parameters depends mainly on the application. Among the useful kernel functions are radial basis functions (RBFs) and polynomial kernel functions. The formulas of these kernel functions are shown below respectively:

$$\left\{ \frac{-|x - xi|^2}{2\sigma^2} \right\} \tag{5}$$

$$[(x^* x_i) + 1]^d \tag{6}$$

where "σ" and "d" are kernel width and order respectively which were experimentally defined to achieve the best classification result. In this work, RBFs and polynomial kernel functions were used with different sigma values (σ = 1.5–4) and orders (d = 1, 2, 3), respectively [41–47].

Evaluation

Our method was validated on 33 male rats. The ability of the proposed method for identifying 6-OHDA-lesioned rats (Off-Stimulation) was evaluated using accuracy (AC), sensitivity (SN), specificity (SP) and precision (P) [47–52]. In the following Eqs. (7)–(10), TP refers to true positives (correctly detected Off-Stimulation), TN refers to true negatives (correctly detected sham), FN refers to false negatives (incorrectly detected sham) and FP refers to false positives (incorrectly predicted Off-Stimulation).

To evaluate the proposed method, AC, SN, SP and P were computed for MLP and SVM classifiers (to evaluate the robustness of the system, this procedure is repeated 10 times).

Accuracy (AC): the ratio of the number of correct classification to the total number of classification.

$$AC = \frac{TP + TN}{TP+TN + FN+FP} \tag{7}$$

Sensitivity (SN): the ratio of true positives to the patient (Off-Stimulation) group.

$$SN = \frac{TP}{FN + TP} \tag{8}$$

Specificity (SP): the ratio of true negatives to the sham group.

$$SP = \frac{TN}{TN + FP} \tag{9}$$

Precision (P): the ratio of the Off-Stimulation detection that were correct

$$P = \frac{TP}{FP + TP} \tag{10}$$

Table 2
Performance of the SVM classifier with different parameters.

Classifier	Accuracy (%)	Sensitivity (%)	Specificity (%)	Precision (%)
SVM-Poly (d = 1)	78.37	15.91	97.85	69.78
SVM-Poly (d = 2)	79.34	56.93	86.93	59.55
SVM-Poly (d = 3)	43.99	79.74	32.17	28.00
SVM-RBF (σ = 1.5)	75.36	3.74	99.09	57.50
SVM-RBF (σ = 2)	76.67	10.07	98.55	69.49
SVM-RBF (σ = 3)	78.82	28.78	95.52	68.20
SVM-RBF (σ = 3.5)	78.21	29.79	95.60	70.86
SVM-RBF (σ = 4)	78.76	31.64	95.56	71.73
SVM-RBF (auto) (σ = 3.65)	80.42	34.62	95.89	73.79
SVM-RBF (auto) (σ = 3.68)	80.31	33.77	95.67	72.00

Results

To optimize the learning cost and the prediction performance, the SVM classifier parameters and kernel width σ must be chosen with more care and caution. To this end, we compared the performance of the networks by evaluating the error function using an independent validation set, and selected the network which has the smallest error with respect to the validation set. Since this procedure can itself lead to some over-fitting to the validation set, the performance of the selected network was confirmed by test data set. In fact, we have divided the training data into train and validation sets with the proportions being 70% & 30% for training and validation datasets respectively.

We have evaluated the performance of the SVM classifier with different kernels, such as polynomials with order 1, 2, and 3 and RBFs with different sigma values (σ = 1.5, 2, 3, 3.47, 3.5, 3.65, 3.68, 4). The optimum values of the parameters, chosen when the error on the validation dataset reaches a minimum, were achieved as 3.65 and 2 for σ and order (d), respectively. To evaluate the performance of the proposed method, four measures were calculated based on Eqs. (7)–(10). The results of classification parameters of test data for each class are summarized in Table 2.

Table 3 summarizes the performance of the two classifiers, i.e. SVM and MLP. Since the best SVM structure were achieved through RBF kernel and automated chosen σ, the average of the last two rows were used for further evaluations. The obtained accuracy, sensitivity, specificity, and precision of the proposed method by SVM, as shown in Table 3, were achieved as 80.42%, 34.62%, 95.89% and 73.79%, respectively. As it was clearly observed in Table 3, the SVM presents better results than MLP; consequently the following investigations were done by SVM.

As previously mentioned, a total of sixty-six features were extracted from the recorded data, out of which thirty-eight were related to low-frequency data while twenty-eight features were associated with high-frequency data. Because of the large number of extracted features and for achieving higher accuracy of classification, GA was employed to find the optimum features desirable. Binary chromosomes should be selected by the number of genes which equals that of the attributes (n = 66) in order to use GA for choosing a feature, in which case, the mode of 1 of the genes means selecting the corresponding feature while 0 implies the lack of selection of the related feature. After implementing GA on a total of sixty-six features, the accuracy of the classifier reached 84.41%, and 38 out of 66 features were selected. Among the 38 selected features, 14 of them were related to low-frequency data whereas 24 of features were associated with high-frequency data. The selected low-frequency features included the three larger local maxima of power spectrum, the amplitude of the 6th peak of the power spectrum, the fifth normalized peak of power spectrum, the amplitude of the two local peaks of power spectrum (with respect to frequency of the occurrence), the fifth amplitude, as well as the sixth and seventh local peak power spectrum (with respect to frequency of the occurrence), the location of the first three peaks of the power spectrum, and finally, the average amplitude of the power spectrum. On the other hand, unselected high-frequency features encompassed the second maxima of the power spectrum, the frequency of the occurrence of the third and fourth larger maxima of the power spectrum, and the amplitude of the first peak of the power spectrum (with respect to frequency of the occurrence), and the remaining twenty-four features were selected.

Table 3
Results of the classifiers performance in percentage.

Classifier	Accuracy (%)	Sensitivity (%)	Specificity (%)	Precision (%)
SVM	80.42	34.62	95.89	73.79
MLP	73.23	65.17	75.99	47.84

The steps for selecting the features and categorizing the dataset at high and low frequencies were separately examined since most of the selected features were related to the high-frequency dataset, and the results were as follows:

- High-frequency Information

Through all high-frequency features and SVM classifier, the accuracy was 78.6%; When 21 of 28 features were selected using the GA and SVM classifier the accuracy was obtained 80.34%.

- Low-frequency Information

Through all low-frequency features and SVM classifier, the accuracy was equal to 75.26%;

When 24 of 38 features were chosen using the GA and SVM classifier the accuracy was obtained 77.73%.

Table 4 presents the results of using GA for choosing the optimal feature classification for separating the two studied groups with the highest intended accuracy. According to these results, combined features of high and low frequencies domains of dataset were employed. In the next study the effect of different stimulation parameters on these features will be investigated. Feature changes of 6-OHDA-lesioned rats using different stimulation protocol and bringing them close to those of sham group will be presented.

Discussion

Nowadays, DBS plays a major role in the treatment of Parkinson's disease. Adjusting the stimulation parameters and their appropriate alteration with disease progression has so far been the subject of various studies while it has not yet been applied. A lot of researches have been done on analyzing LFPs. One of the basis application for signal processing is transition from time to the frequency domain [53]. Various studies have mainly focused on monitoring beta band LFP only [17,54,55]. However, using only beta band LFP may not be sufficient, as they have not displayed satisfactory consistency across time and patients [54,56]. The correlation of gamma [33,57,58], and tremor

Table 4
The Classification Accuracy of SVM with and without GA in Sham and Off-Stimulation Groups.

	Classification Accuracy with SVM/without GA	Classification AccuracywithSVM and GA	The Number of Selected Features by GA
High-frequency data	78.60	80.34	21 of 28 features
Low-frequency data	75.26	77.73	24 of 38 features
A combination of high and low frequency	80.42	84.41	38 of 66 features

[59] bands with PD symptoms were the subjects of some other researchers which impressed suitability of using beta band activities alone. There were researches which have used the wavelet transformation in LFP processing [60] and also some other time–frequency transformation algorithms like Hilbert's transform used for the analysis of LFP [61]. On the other hand, the relationship of the LFPs from different sources was analyzed, and the results were used as biomarkers for the closed-loop DSB system [62–67].

In the present study, the recorded and evaluated LFP signals of rats provide the prologue for selecting the appropriate biomarker and extracting the features in order to make the closed-loop DBS. After investigating the data related in the frequency domain for sham and Off-Stimulation groups, it was detected that the LFP features were able to separate the sham group from the patient group (Off-Stimulation) with an approximate accuracy of 84%. This implies that the LFP signal can convincingly feedback the disease states.

Investigating the frequency domain features extracted from the LFP signal in both high- and low-frequency band (above and below 100 Hz) strongly suggests that frequency domain of LFPs contain important information for representing the state of the disease. Since most studies focused on analyzing LFPs in low-frequency domain, selecting the majority of the extracted features by GA from high-frequency compared to low-frequency data is highly important and it illustrate high-frequency domain should be studied more precisely. The results further revealed that high-frequency data could alone distinguish the sham group from Off-Stimulation group with an approximate accuracy of 80%. Since rats LFP signals were investigated in this study and motor symptoms in rats are not same as in human, we cannot discuss whether or not the differences in high- and low-frequency were related to motor disorders; nevertheless, LFP meaningful changes in unhealthy rats were obvious and varied as DBS was applied. Studying the averages of the selected features in two groups, we realized that among all the features selected through GA, those chosen as the locations of local maxima in PSD (occurrence frequencies) in high frequency were all above 200 Hz being generally in range of 200, 600 and above 1000 Hz. These frequencies in low-frequency portion were below 10, 31–47 and 57–62 Hz. We can therefore conclude that it is worthwhile to have these frequency ranges more carefully reviewed. We drew a comparison between the features selected by GA when the classifier used only high- or low-frequency features and when it applied a combination of high- and low-frequency features and noticed a number of differences and similarities. Some feature were selected in high- or low-frequency classification which they weren't in combination condition and vice versa. Statistically, 58% of selected features in low-frequency classification were not included in the combination mode while this percentage for high-frequency classification was only 9%. 28% of selected low-frequency information in the combination mode were new in comparison with low-frequency classification while this number was as low as 16% for high-frequency information. These numbers indicate that high-frequency information have more robustness in classification of sham and 6-OHDA-lesioned rats.

Conclusion

The frequency features extracted from the LFP signals have ability to separate parkinsonian rats from healthy ones reasonably; when stimulation was given to parkinsonian rat model, these features came close to ones of sham group so they can be introduced as appropriate biomarkers for closed-loop DBS.

Declaration of Competing Interest

The authors declare that they have no known competing financial interests or personal relationships that could have appeared to influence the work reported in this paper.

Appendix A. Supplementary data

Supplementary data to this article can be found online at https://doi.org/10.1016/j.mehy.2019.109360.

References

[1] Mehanna R, Lai CE. Deep brain stimulation for Parkinson's disease. Transl Neurodegener 2013;22(2):1–10. https://doi.org/10.1186/2047-9158-2-22.
[2] Jankovic J. Parkinson's disease: clinical features and diagnosis. J Neurol Neurosurg Psychiatry 2008;79(4):368–76. https://doi.org/10.1136/jnnp.2007.131045.
[3] Chinta SJ, Andersen JK. Dopaminergic neurons. Int J Biochem Cell Biol 2004;37(5):942–6. https://doi.org/10.1016/j.biocel.2004.09.009.
[4] Rabey JM, Hefti F. Neuromelanin synthesis in rat and human substantia nigra. J Neural Trans – Parkinson's Dis Dementia Sect 1990;2(1):1–14.
[5] Alves G, Wentzel-Larsen T, Larsen JP. Is fatigue an independent and persistent symptom in patients with Parkinson disease? Neurology 2004;63(10):1908–11. https://doi.org/10.1212/01.wnl.0000144277.06917.cc.
[6] Kringelbach ML, Jenkinson N, Owen SL, Aziz TZ. Translational principles of deep brain stimulation. Nat Rev Neurosci 2007 Aug;8(8):623–35. https://doi.org/10.1038/nrn2196.
[7] Breit S, Schulz JB, Benabid AL. Deep brain stimulation. Cell Tissue Res 2004;318(1):275–88.
[8] Priori A, Foffani G, Rossi L, Marceglia S. Adaptive deep brain stimulation (aDBS) controlled by local field potential oscillations. Exp Neurol 2013;245:77–86. https://doi.org/10.1016/j.expneurol.2012.09.013.
[9] Bronstein JM, Tagliati M, Alterman RL, et al. Deep brain stimulation for Parkinson disease: an expert consensus and review of key issues. Archiv Neurol 2011;68(2):165. https://doi.org/10.1001/archneurol.2010.260.
[10] Parastarfeizabadi M, Kouzani AZ. Advances in closed-loop deep brain stimulation devices. J Neuro Eng Rehabil 2017;14(1):79. https://doi.org/10.1186/s12984-017-0295-1.
[11] Kuo CH, White-Dzuro GA, Ko AL. Approaches to closed-loop deep brain stimulation for movement disorders. Neurosurg Focus 2018;45(2):E2. https://doi.org/10.3171/2018.5.FOCUS18173.
[12] Priori A, Foffani G, Pesenti A, et al. Rhythm-specific pharmacological modulation of subthalamic activity in Parkinson's disease. Exp Neurol 2004;189(2):369–79. https://doi.org/10.1016/j.expneurol.2004.06.001.
[13] Priori A, Foffani G, Rossi L. Apparatus for treating neurological disorders by means of adaptive electro-stimulation retroacted by biopotentials. US Patent 8,078,281; 28.10. 2005.
[14] Wingeier B, Tcheng T, Koop MM, Hill BC, Heit G, Bronte-Stewart HM. Intra-operative STN DBS attenuates the prominent beta rhythm in the STN in Parkinson's disease. Exp Neurol 2006;197(1):244–51. https://doi.org/10.1016/j.expneurol.2005.09.016.
[15] Rosin B, Slovik M, Mitelman R, et al. Closed-loop deep brain stimulation is superior in ameliorating parkinsonism. Neuron 2011 Oct 20;72(2):370–84. https://doi.org/10.1016/j.neuron.2011.08.023. doi: 10.1016/j.neuron.2011.08.023.
[16] Santaniello S, Fiengo G, Glielmo L. Closed loop control of deep brain stimulation: a simulation study. IEEE Trans Neural Syst Rehabil Eng 2011;19(1):15–24.
[17] Grant PF, Lowery MM. Simulation of cortico-basal ganglia oscillations and their suppression by closed loop deep brain stimulation. IEEE Trans Neural Syst Rehabil Eng 2013;21(4):584–94. https://doi.org/10.1109/TNSRE.2012.2202403.
[18] Basu I, Graupe D, Tuninetti D, et al. Pathological tremor prediction using surface electromyogram and acceleration: potential use in 'ON–OFF' demand driven deep brain stimulator design. J Neural Eng 2013;10(3):19–36. https://doi.org/10.1088/1741-2560/10/3/036019.
[19] Kent AR, Grill WM. Recording evoked potentials during deep brain stimulation: development and validation of instrumentation to suppress the stimulus artefact. J Neural Eng 2012;9(3):036004https://doi.org/10.1088/1741-2560/9/3/036004.
[20] Kent AR, Grill WM. Neural origin of evoked potentials during thalamic deep brain

stimulation. J Neurophysiol 2013;110(4):826–43.
[21] Gmel EG, Parker JL, Obradovic M, et al. Recording Fast Responses and Late Responses during Deep Brain Stimulation in patients with Parkinson's disease. In: The 3rd International Conference on Medical Bionics, Phillip Island, Victoria, Australia; 2013.
[22] Gmel GE, Parker JL, Hamilton TJ. A new biomarker for closed-loop deep brain stimulation in the subthalamic nucleus for patients with Parkinson's disease. In: Biomedical Circuits and Systems Conference (BioCAS), 2014 IEEE, Lausanne, 2014. Doi: 10.1109/BioCAS.2014.6981772.
[23] Weinberger M, Hutchison WD, Dostrovsky JO. Pathological subthalamic nucleus oscillations in PD: can they be the cause of bradykinesia and akinesia? Exp Neurol 2009;219(1):58–61. https://doi.org/10.1016/j.expneurol.2009.05.014.
[24] Brown P. Oscillatory nature of human basal ganglia activity: relationship to the pathophysiology of Parkinson's disease. Mov Disord 2003;18(4):357–63.
[25] Liu J, Khalil HK, Owies KG. Model-based analysis and control of a network of basal ganglia spiking neurons in the normal and Parkinsonian states. J Neural Eng 2011;8(4):1–27. https://doi.org/10.1088/1741-2560/8/4/045002.
[26] Marceglia S, Fumagalli M, Priori A. What neurophysiological recordings tell us about cognitive and behavioral functions of the human subthalamic nucleus. Expert Rev Neurother 2011;11(1):139–49. https://doi.org/10.1586/ern.10.184.
[27] Winestone JS, Zaidel A, Bergmand H, Israel Z. The use of macroelectrodes in recording cellular spiking activity. J Neurosci Meth 2012;206(1):34–9. https://doi.org/10.1016/j.jneumeth.2012.02.002.
[28] Rouse AG, Stanslaski SR, Cong P, et al. Denison. A chronic generalized bi-directional brain–machine interface. J Neural Eng 2011;8(3):1–19. https://doi.org/10.1088/1741-2560/8/3/036018.
[29] Marceglia S, Rossi L, Foffani G, Bianchi A, Cerutti S, Priori A. Basal ganglia local field potentials: applications in the development of new deep brain stimulation devices for movement disorders. Exp Rev Med Dev 2007;4(5):605–14.
[30] Quinn EJ, Blumenfeld Z, Velisar A, et al. Beta oscillations in freely moving Parkinson's subjects are attenuated during deep brain stimulation. Mov Disord 2015;30(13):1750–8. https://doi.org/10.1002/mds.26376.
[31] Niketeghad S, Hebb AO, Nedrud J, Hanrahan SJ, Mahoor MH. Single trial behavioral task classification using subthalamic nucleus local field potential signals. In: Annual International Conference of the IEEE Engineering in Medicine and Biology Society, Chicago, 2014;3793-3796. doi: 10.1109/EMBC.2014.6944449.
[32] Mamun KA, Mace M, Lutman ME, et al. Movement decoding using neural synchronization and inter-hemispheric connectivity from deep brain local field potentials. J Neural Eng 2015;12(5):1–18. https://doi.org/10.1088/1741-2560/12/5/056011.
[33] Brown P, Williams D. Basal ganglia local field potential activity: character and functional significance in the human. Clin Neurophysiol 2005;116(11):2510–9.
[34] Ebrahimzadeh E, Pooyan M. Early detection of sudden cardiac death by using classical linear techniques and time-frequency methods on electrocardiogram signals. J Biomed Sci Eng Pap Submission 2011;4(11):699–706.
[35] Ebrahimzadeh E, Pooyan M, Bijar A. A novel approach to predict sudden cardiac death (SCD) using nonlinear and time-frequency analyses from HRV signals. PLoS One 2014;9(2):1–14. https://doi.org/10.1371/journal.pone.0081896.
[36] Ebrahimzadeh E, Pooyan M, Jahani S, Bijar A, Setaredan S. ECG signal noise removal: selection and optimization of the best adaptive filtering algorithm based on various algorithms comparison. Biomed Eng: Appl Basis Commun 2015;27(4):1–13. https://doi.org/10.4015/S1016237215500386.
[37] Ebrahimzadeh E, Fayaz F, Ahmadi F, Nikravan M. A machine learning-based method in order to diagnose lumbar disc herniation disease by MR image processing. Med Life Open Access 2018;1:1–10.
[38] Ebrahimzadeh E, Fayaz F, Ahmadi F, Rahimidolatabad M. Linear and nonlinear analyses for detection of sudden cardiac death (SCD) using ECG and HRV signals. Trends Res 2018;l(1):1–8. https://doi.org/10.15761/TR.1000105.
[39] Ebrahimzadeh E, Soltanian_Zadeh H, Araabi BN. Localization of epileptic focus using simultaneously acquired EEG-FMRI data. Comput Intell Electr Eng 2018;9(2):15–28.
[40] Ebrahimzadeh E, Araabi BN. A novel approach to predict sudden cardiac death using local feature selection and mixture of expert. PLoS One 2014;9(2):1–14. https://doi.org/10.1371/journal.pone.0081896.
[41] Amoozegar S, Pooyan M, Ebrahimzadeh E. Classification of brain signals in normal subjects and patients with epilepsy using mixture of experts. Int J Eng Intell Syst Electr Eng Commun 2013;4(1):1–8.
[42] Ebrahimzadeh E, Alavi SM, Bijar A, Pakkhesal A. A novel approach for detection of deception using Smoothed Pseudo Wigner-Ville Distribution (SPWVD). J Biomed Sci Eng 2013;6(1):8–18.
[43] Ebrahimzadeh E, Alavi SM, Samsami K. Implementation and designing of lie-detection system based on Electroencephalography (EEG). Annal Military Health Sci Res 2013;11(1):20–6.
[44] Ebrahimzadeh E, Foroutan A, Shams M, et al. An optimal strategy for prediction of sudden cardiac death through a pioneering feature-selection approach from HRV signal. Comput Meth Programs Biomed 2019;169:19–36.
[45] Rahimpour A, Noubari HA, Kazemian M. A case-study of NIRS application for infant cerebral hemodynamic monitoring: a report of data analysis for feature extraction and infant classification into healthy and unhealthy. Inf Med Unlocked 2018;11:44–50.
[46] Ebrahimzadeh E, Pooyan M. Prediction of sudden cardiac death (SCD) using time-frequency analysis of ECG signals. Comput Intell 2013;3(4):15–26.
[47] Ebrahimzadeh E, Manouchehri MS, Amoozegar S, Araabi BN, Soltanian-Zade H. A time local subset feature selection for prediction of sudden cardiac death from ECG signal. Med Biol Eng Comput 2017;56(7):1253–70.
[48] Nikravan M, Ebrahimzadeh E, Izadi MR, Mikaeili M. Towards an automatic diagnosis system for lumbar disc herniation: the significance of local subset feature. Biomed Eng: Appl Basis Commun 2016;28(6):1–10. https://doi.org/10.4015/S1016237218500448.
[49] Ebrahimzadeh E, Soltanian-Zadeh H, Araabi BN, Fesharaki SSH, Habibabadi JM. Component-related BOLD response to localize epileptic focus using simultaneous EEG-fMRI recordings at 3T. J Neurosci Meth 2019;334:34–49.
[50] Ebrahimzadeh E, Kalantari M, Joulani M, Shahraki RS, Fayaz F, Ahmadi F. Prediction of paroxysmal Atrial Fibrillation: a machine learning based approach using combined feature vector and mixture of expert classification on HRV signal. Comput Methods Programs Biomed 2018;165:53–67.
[51] Rahimpour A, Dadashi A, Soltanian-Zadeh H, Setarehdan SK. Classification of fNIRS based brain hemodynamic response to mental arithmetic tasks. IEEE; 2017. p. 113–7.
[52] Ebrahimzadeh E, Shams M, Fayaz F, Rajabion L, Mirbagheri M, Araabi BN, et al. Quantitative determination of concordance in localizing epileptic focus by component-based EEG-fMRI. Comput Meth Programs Biomed 2019;177:231–41.
[53] Michmizos KP, Sakas D, Nikita KS. Prediction of the timing and the rhythm of the Parkinsonian subthalamic nucleus neural spikes using the local field potentials. IEEE Trans Biomed Eng 2012;16(2):190–7.
[54] Little S, Pogosyan A, Neal S, Zavala B, Zrinzo L, Hariz M, et al. Adaptive deep brain stimulation in advanced Parkinson disease. Ann Neurol 2013;74(3):449–57. https://doi.org/10.1002/ana.23951.
[55] Little S, Pogosyan A, Kuhn AA, Brown P. β band stability over time correlates with Parkinsonian rigidity and bradykinesia. Exp Neurol 2012;236(2):383–8. https://doi.org/10.1016/j.expneurol.2012.04.024.
[56] Alegre M, Valencia M. Oscillatory activity in the human basal ganglia: more than just beta, more than just Parkinson's disease. Exp Neurol 2013;248:183–6. https://doi.org/10.1016/j.expneurol.2013.05.018.
[57] Little S, Brown P. What brain signals are suitable for feedback control of deep brain stimulation in Parkinson's disease? Ann N Y Acad Sci 2012;1265(1):9–24. https://doi.org/10.1111/j.1749-6632.2012.06650.x.
[58] Brittain JS, Brown P. Oscillations and the basal ganglia: motor control and beyond. NeuroImage 2014;85(2):637–47. https://doi.org/10.1016/j.neuroimage.2013.05.084.
[59] Heida T, Wentink EC, Marani E. Power spectral density analysis of physiological, rest and action tremor in Parkinson's disease patients treated with deep brain stimulation. J Neuro Eng Rehabil 2013;10(1):70. https://doi.org/10.1186/1743-0003-10-70.
[60] Mohammed A, Zamani M, Bayford R, Demosthenous A. Toward On-demand deep brain stimulation using online Parkinson's Disease prediction driven by dynamic detection. IEEE Trans Neural Syst Rehabil Eng 2017;25(12):2441–52.
[61] Zhao D, Sun Q, Cheng S, He M, Chen X, Hou X. Extraction of Parkinson's disease-related features from local field potentials for adaptive deep brain stimulation. Neurophysiology 2018;1:57–67.
[62] Liu C, Wang J, Deng B, Wei XL, Yu HT, Li HY. Variable universe fuzzy closed-loop control of tremor predominant Parkinsonian state based on parameter estimation. Neurocomputing 2015;151(3):1507–18.
[63] Bandopadhyay R. Sequential extraction of soluble and insoluble alpha-synuclein from Parkinsonian brains. J Visualized Exp 2016;107:1–6. https://doi.org/10.3791/53415.
[64] Ertuğrul ÖF, Kaya Y, Tekin R, Almali MN. Detection of Parkinson's disease by shifted one dimensional local binary patterns from gait. Expert Syst Appl 2016;56:156–63.
[65] Pan S, Iplikci S, Warwick K, Aziz T. Parkinson's disease tremor classification – a comparison between Support Vector Machines and neural networks. Expert Syst Appl 2012;39(12):10764–71.
[66] Hohlefeld FU, Huebl J, Huchzermeyer C, Schneider GH, Schönecker T, Kühn AA, et al. Long-range temporal correlations in the subthalamic nucleus of patients with Parkinson's disease. Eur J Neurosci 2012;36(6):2812–21. https://doi.org/10.1111/j.1460-9568.2012.08198.x.
[67] Connolly AT, Muralidharan A, Hendrix C, Johnson L, Gupta R, Stanslaski S, et al. Local field potential recordings in a non-human primate model of Parkinsons disease using the activa PC neurostimulator. J Neural Eng 2015;12(6):1–25. https://doi.org/10.1088/1741-2560/12/6/066012.